



Correlation Analysis of Breast Cancer DWI Combined with DCE-MRI Imaging Features with Molecular Subtypes and Prognostic Factors

Congru Yuan¹ · Feng Jin² · Xiuling Guo² · Sheng Zhao² · Wei Li³ · Haidong Guo²

Received: 26 December 2018 / Accepted: 3 February 2019 / Published online: 27 February 2019
© Springer Science+Business Media, LLC, part of Springer Nature 2019

Abstract

This study aimed to deeply analyze the application of DWI and DCE-MRI imaging in breast cancer, the correlation between the imaging characteristics of DWI and DCE-MRI and the molecular subtypes and prognostic factors of breast cancer was studied. Firstly, DWI and DCE-MRI scans of all patients before interventional therapy were performed, and relevant information of the subjects was introduced in turn. Secondly, molecular subtypes were determined according to immunohistochemical results and gene amplification. Siemens 3.0 T post-processing workstation was used for image post-processing. The time signal curve (TIC), early enhancement rate (EER) and ADC values were measured, morphological characteristics were recorded, and the correlation between each image feature and molecular subtypes, prognostic factors (tumor size, pathological grade, lymph node metastasis, ER, PR, HER2, Ki67) was analyzed. The results showed that parameters such as ADC value, EER, lobulation sign, burr sign, enhancement way and TIC type were correlated with prognostic factors and molecular subtypes. And Bayesian model discriminant analysis showed that the above imaging parameters couldn't well predict the expression of immunohistochemical factors and molecular subtypes. However, the above characteristics had a good effect on the prediction of pathological grade, with a false diagnosis rate of 9.69%.

Keywords Breast cancer · Diffusion-weighted imaging · DCE-MRI · Molecular subtype · Prognostic factor

Introduction

In recent years, breast cancer has been considered to be a biologically heterogeneous tumor. It includes different subtypes, presenting with different natural histories of disease and clinical outcomes [1, 2]. Studies have found that even patients with the same anatomical and pathological risk factors have differences in their natural history of disease and

treatment response, most of which are due to molecular heterogeneity [3–5]. Therefore, the exploration of molecular markers has become a major focus. The ability of these molecular markers to predict prognosis and response to treatment is assessed to help develop individualized treatment options for breast cancer patients.

In recent years, many studies have explored the value of molecular prognostic markers and found oncogenes and tumor suppressor genes through the molecular studies of tumors [6, 7]. In practice, pathologists use immunohistochemistry (IHC) or immunocytochemistry to detect the protein products of these genes. Biomarkers have potential significance in identifying different histopathological types of breast cancer, assessing prognosis and predicting response to undetermined systemic therapy. Typical biomarkers have continuous clinical value, while the subjective setting of the boundary value is mainly to simplify clinical treatment. The goal of the boundary value setting should be to prevent patients from producing too many or too few clinical subtypes, so as not to lead to too much or insufficient treatment in the future [8]. In this study, the dynamic enhancement and diffusion weighted imaging manifestations of breast cancer were observed, the correlation

This article is part of the Topical Collection on *Image & Signal Processing*

✉ Haidong Guo
guohaidonghd00@163.com

¹ Department of Geriatrics, The Affiliated Hospital of Inner Mongolia Medical University, Huhhot 010110, Inner Mongolia, China

² Department of Radiology, The Affiliated Hospital of Inner Mongolia Medical University, No. 1 Tongdao North Road, Huimin District, Hohhot 010110, Inner Mongolia, China

³ Department of Radiology, The Second Affiliated Hospital of Inner Mongolia Medical University, Huhhot 010030, Inner Mongolia, China

between DCE-MRI, DWI manifestations and biological prognostic factors of breast cancer was preliminarily analyzed, and the feasibility of MRI in the preoperative evaluation of prognosis of breast cancer was discussed, providing basis for early diagnosis of breast cancer, reasonable formulation of treatment scheme and prognosis evaluation.

Methods and materials

Object of study

196 cases of breast cancer patients diagnosed in The Affiliated Hospital of Inner Mongolia Medical University from August 2013 to January 2018 were collected, and all enrolled patients signed informed consent before MRI examination. This study was approved by the Ethics Committee of The Affiliated Hospital of Inner Mongolia Medical University. The inclusion conditions were: the patients underwent conventional MRI, DWI and DCE-MRI scans at the same time; no surgery, radiotherapy, chemotherapy, and core puncture biopsy were performed before the examination; the patient had complete surgical pathology, immunohistochemical results and metastasis of sentinel and axillary lymph node; MRI inspection image was complete, in line with routine diagnostic needs. Those who don't meet the above conditions were excluded.

The mean age of 196 patients was 47.6 ± 9.5 years old, all of which were unilateral breast lesions (10 patients had a history of contralateral breast cancer surgery). The number of different molecular subtypes was 38 cases (19.4%) of Luminal A, 110 cases (56.1%) of Luminal B, 30 cases (15.3%) of HER2 overexpression and 18 cases (9.2%) of Basal-like.

The prognostic factors were statistically analyzed: pathological grades were divided into high-invasive group (grade II, grade III) and low-invasive group (intraductal carcinoma, grade I); Ki67 was divided into high expression group ($> 14\%$) and low expression group ($\leq 14\%$); axillary lymph node metastasis, ER, PR and HER2 were divided into positive group and negative group respectively.

Photographic methods

MRI scanning was performed with SIEMENS 3.0 T magnetic resonance imaging (SIEMENS 3.0 TVERIO) and dedicated breast coil for data collection. The patient was in a prone position with both breasts hanging naturally in the breast coil; after scanning and positioning, transverse axis fat inhibition FSE sequence T2WI, DWI and multi-phase dynamic enhanced scanning were performed, respectively.

DWI parameters were as follows: TR/TE: 5300/90 ms; FOV: 35×35 cm; matrix: 192×192 ; layer thickness/interval:

4 mm/2 mm; b value: 0, 700, and 1000; excitation times: 8; scanning time: 5 min and 13 s.

DCE-MRI scanning used 3DT1-weighted sequence axial scanning, a total of 6 phases (The first phase was plain scan of the mask, At the end of the first phase, enhancement scan was performed at the last 5 phases). Scanning parameters were as follows: TR/TE: 4.32/1.57 ms, flip angle (FA): 10° , FOV: 34×34 cm, matrix: 448×448 , incentive number: 1, the layer thickness: 1 mm, unspaced scanning, the scan time of each period was 1 min and 7 s, and the total scan time was 7 min and 2 s. Gadopentetate dimeglumine pentaacetic acid (Gd-DTPA) was used as the contrast enhancement agent at a dose of 0.1 mmol/Kg, which was injected at a speed of 3.0 ml/s through the elbow vein.

Image analysis and post-processing methods

DWI and DCE-MR scan data were analyzed with SIEMENS post-processing workstation. Combined with T2WI fat suppression sequence and DCE-MRI image, an experienced radiologist manually delineated the Region of Interest (ROI) at the maximum level of the lesion in the ADC image. Its size was about 0.3cm^2 , avoiding obvious necrosis, hemorrhage and cystic changes. It was measured in the low signal and uniform area, and the mean value was obtained after repeated measurement for 3 times. TIC measurement: in the largest level of dynamic enhancement map lesions, ROI selected the most prominent area of enhancement, avoiding obvious bleeding and necrotic areas. Finally, the morphological manifestations, enhancement types, and TIC types of the lesions were analyzed and recorded (Fig. 1).

Pathological results and molecular typing methods

According to the postoperative pathological sections and immunohistochemical results of professional pathologists, the pathological grade of tumors, axillary lymph node metastasis and immunohistochemical factor expression are obtained, so as to determine the molecular subtype of breast cancer. Pathological grade is assessed with the Elston-Ellis system, and the assessment includes the formation proportion of gland and glandular tube, nuclear pleomorphism, and mitotic count. Each factor is independently evaluated with 1–3 points, and the final score is combined to determine the grading. Among them, level I: 3–5 points; level II: 6–7 points; level III: 8–9 points. Immunohistochemical results are determined according to the relevant guideline standards, and ER and PR criteria are determined according to the "ASCO/CAP Breast Cancer Hormone Receptor IHC Detection Guide". The nucleus staining of $\geq 1\%$ of the tumor cells is defined as positive, and vice versa. HER2 criteria refer to the "Breast Cancer HER2 Detection Guidelines". When

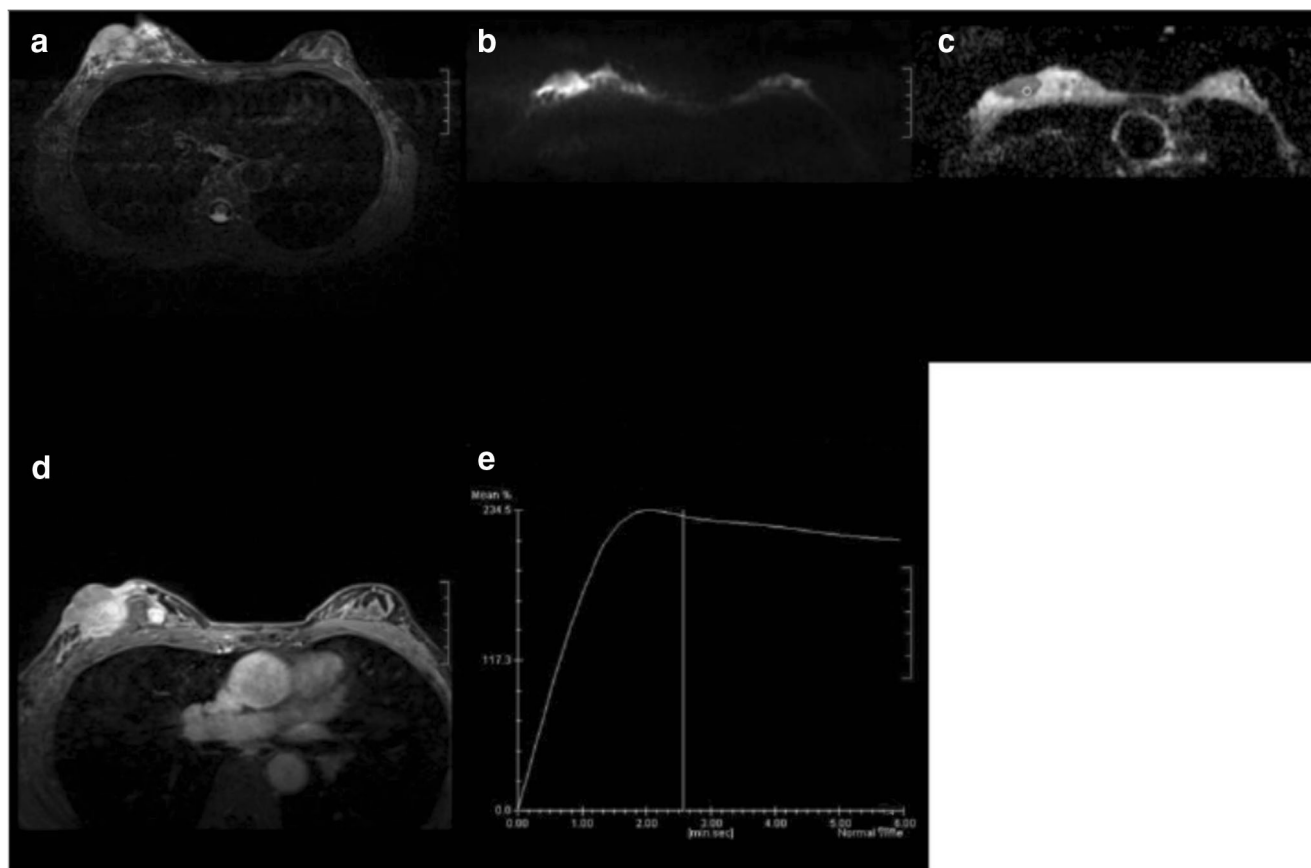


Fig. 1 Measurement of ADC value and TIC. Female patient, 45 years old, with a right invasive ductal carcinoma grade III and HER2 overexpression. A: a round mass in the outer upper quadrant of the right breast with a clear border. B: the DWI shows uneven high signal. C: ADC value was measured, the largest lesion layer was selected, and

the lower signal area was measured with a small ROI. D~E: dynamically enhanced TIC curve measurement selected the largest level of lesions, the most obvious enhancement zone was measured with a small ROI, and the lesion TIC was type II.

the expression is (3+), it is positive; when the expression is (2+), further FISH detection of gene amplification is required, and if it is amplified, it is positive, and vice versa. Molecular subtypes are judged according to the standards in “China Anti-Cancer Association Breast Cancer Treatment Guidelines and Regulations (2015 Edition)”: Luminal A: ER/PR(+) and high PR expression (>20%), HER2(-), low Ki67 expression (\leq 14%); Luminal B (HER2 negative): ER/PR (+), HER2 (-), and low expression of PR (< 20%) or high expression of Ki67 (> 14%); Luminal B (HER2 positive): ER/PR (+), HER2 (+), Ki67 (\pm); ERBB2+: HER2 (+), ER (-), PR (-); Basal-like (three negative non-specific invasive ductal carcinoma): ER, PR, and HER2 are all negative. Luminal B subtype is not classified as independent.

DWI imaging technology

DWI is the only imaging method that can observe the microscopic motion of living water molecules, namely Brownian motion [9]. It reflects the spatial composition

information of human tissues and the functional changes of water molecules in various tissue components under pathophysiological state at the molecular level and can detect the early morphological and physiological changes related to the changes of moisture content of tissue, so as to provide information for the diagnosis of lesions and differential diagnosis [10]. 70% of water in human body exists in intracellular, extracellular and between tissues, among which the molecule movement of extracellular water has the greatest impact on DWI. DWI uses a pair of diffusion sensitive gradients with the same amplitude and opposite direction to phase shift the hydrogen protons. The freer the water molecules in the tissue, the more discrete the intermolecular phase, and the lower the intensity of the acquired signal. Diffusion imaging is highly sensitive to movement. In this complex environment in the body, voluntary or involuntary movements such as heartbeat, pulse, respiration and blood perfusion can lead to decreased DWI signal. Therefore, in clinical application, the Apparent Diffusion Coefficient (ADC) is often used to represent the diffusion coefficient. The ADC formula is as follows:

$$ADC = [\ln(S_{low}-S_{high})]/(b_{high}-b_{low}) \quad (1)$$

Where, S_{low} and S_{high} respectively represent the signal intensity values measured by low b value and high b value diffusion imaging, which can be measured from the region of interest set on the image. ADC is affected by a variety of factors. In addition to the most important tissue characteristics, ADC is also affected by MRI equipment and b value. Among them, b value is an important parameter of imaging. B value is the diffusion sensitivity coefficient, which determines the sensitivity of water molecule diffusion movement, expressed by the following formula:

$$b = \gamma^2 G^2 \delta^2 (\Delta - \delta/3) \quad (2)$$

Among them, γ is the magnetic rotation ratio, G is the intensity of the diffusion gradient, δ represents the duration, Δ is interval time between positive gradient and negative gradient, and the unit is s/mm^2 . The larger the b value is, the more it is biased toward the diffusion image, and the smaller the b value is, the more it is biased toward the T_2 image. Common EPI techniques can freeze most physiological activities, but it can't control blood flow in the tissue. Therefore, the measured ADC values mainly include the thermal motion of water molecules and blood perfusion of tissue.

Results and discussion

Comparison of ADC value and EER between groups of prognostic factors and subtypes

ADC value: the high pathological level group was lower than the low pathological level group: $0.864 \times 10^{-3} \text{ mm}^2/\text{s}$ VS $0.946 \times 10^{-3} \text{ mm}^2/\text{s}$, $P = 0.001$, lymph node metastasis group was lower than non-metastatic group: $0.867 \times 10^{-3} \text{ mm}^2/\text{s}$ VS $0.907 \times 10^{-3} \text{ mm}^2/\text{s}$, $P = 0.013$; EER: higher pathological level group was higher than low pathological level group: 168.3% VS 148.2%, $P = 0.019$; lymph node metastasis group was higher than the negative group: 168.9% VS 160.1%, $P = 0.037$. There was no statistical significance between the groups of residual prognostic factors. The above results were shown in Tables 1 and 2, Figs. 2, 3 and 4.

Comparison of tumor size, lobulation, burr and other morphological characteristics between groups of immunohistochemical factors and subtypes

Tumor size: ER and PR positive groups were smaller than negative groups (2.5 cm VS 3.2 cm, 2.6 cm VS 3.4 cm, $P = 0.001$); HER2: the positive group was larger than the negative group (3.2 cm VS 2.4 cm, $P = 0.034$); Ki67: the high

Table 1 Comparison of ADC value and EERs among all prognostic factors groups

Prognostic factor	Number of cases	ADC value ($\times 10^{-3} \text{ mm}^2/\text{s}$)	P value	EER (%)	P value
Pathological grade					
High grade	174	0.864(0.760, 0.953)	0.001*	168.3(150.0, 188.6)	0.019*
Low grade	22	0.946(0.898, 1.111)		158.4(138.0, 177.1)	
Axillary lymph node					
Positive	114	0.867(0.759, 0.934)	0.013*	168.9(154.9, 191.1)	
Negative	82	0.907(0.798, 1.067)		160.1(142.4, 180.7)	0.037
ER					
Positive	145	0.882(0.785, 0.950)	0.405	170.7 \pm 33.9	0.220
Negative	51	0.883(0.753, 1.082)		164.6 \pm 24.0	
PR					
Positive	134	0.880(0.785, 0.950)	0.480	165.8(151.1, 189.3)	0.345
Negative	62	0.886(0.759, 1.079)		164.9(140.2, 185.6)	
HER2					
Positive	63	0.882(0.761, 1.010)	0.178	164.6(137.8, 186.8)	0.352
Negative	133	0.883(0.791, 0.961)		166.3(150.1, 186.9)	
Ki67					
High expression	143	0.884(0.750, 0.999)	0.461	167.5 \pm 31.0	0.231
Low expression	53	0.886(0.747, 1.008)		169.5 \pm 25.4	

High pathological level group includes II, III grade of patients, low pathological level group includes patients with intraductal carcinoma of grade I; patients with axillary lymph node metastasis were positive, and vice versa; Ki67 is determined according to the standard of "China Anti-Cancer Association Breast Cancer Treatment Guidelines and Regulations (2015 Edition)". If Ki67 expression is greater than 14%, it is high expression, and if it is less than or equal to 14%, it is low expression

*represents $P < 0.05$

Table 2 Comparison of ADC values and EERs among groups of molecular subtypes

Molecular subtype	ADC value ($\times 10^{-3}$ mm ² /s)	P value	EER (%)	P value
Luminal (148) VS	0.883(0.784, 0.950)	0.756	166.1(149.3, 187.7)	0.436
HER2 overexpression (30) Luminal (148)	0.876(0.752, 1.076)	0.369	162.7(137.1, 187.6)	0.697
VS	0.883(0.784, 0.950)		166.1(149.3, 187.7)	
Basal-like (18) HER2(30)	0.893(0.760, 0.953)	0.462	166.9(150.0, 186.8)	0.580
VS	0.876(0.752, 1.076)		162.7(137.1, 187.6)	
Basal-like (18)	0.893(0.760, 0.953)		166.9(150.0, 186.8)	

expression group was larger than the low expression group (2.6 cm VS 2.4 cm, $P = 0.023$). The rate of burr sign in ER and PR positive group was higher than that in negative group, the rate of burr sign in Ki67 low expression group was higher than that in Ki67 high expression group ($p < 0.05$), and the difference was statistically significant. There was no statistically significant difference in the distribution of lobulation between the groups of immunohistochemical factors ($p > 0.05$). The above results were shown in Tables 3 and 4, Figs. 2, 3, and 4.

Correlation analysis of DCE-MRI features, ADC values, prognostic factors and molecular subtypes

ADC value was negatively correlated with pathological grade and lymph node metastasis ($r = -0.265-0.177$, $P = 0.000-0.013$); EER was positively correlated with pathological grade and lymph node metastasis ($P = 0.019-0.037$, $r = 0.168-0.149$); TIC type was positively correlated with HER2 and pathological grade ($P = 0.000-0.001$, $r = 0.228-0.287$); the

tumor size was negatively correlated with ER and PR ($P = 0.000$, $r = -0.289-0.297$); tumor size was positively correlated with high expression of HER2+ and Ki67 ($P = 0.001-0.023$, $r = 0.247-0.162$); tumor size was positively correlated with molecular subtypes ($P = 0.000$, $r = 0.273$); the lobulation sign was positively correlated with pathological grade ($P = 0.001$, $r = 0.264$); the burr sign was positively correlated with the positive expression of ER and PR ($P = 0.001$, $r = 0.298-0.308$), and negatively correlated with the high expression of KI67 ($P = 0.009$, $r = -0.185$); the enhancement way was negatively correlated with positive expression of PR ($P = 0.01$, $r = -0.183$) and positively correlated with high expression of Ki67 ($P = 0.003$, $r = 0.212$). The results were shown in Table 5.

Discriminant analysis results of Bayesian model

The Bayesian discriminant analysis model was established for pathological grade, axillary lymph node metastasis, immunohistochemical factors, and molecular subtypes. The

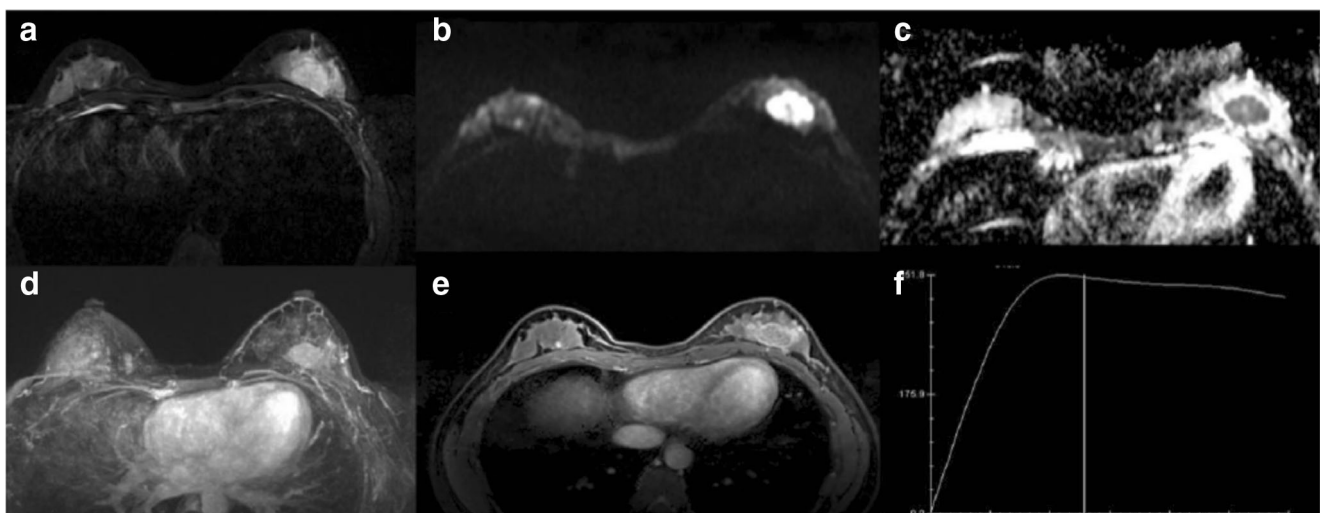


Fig. 2 Female patient, 45 years old, with a grade 3 infiltrating ductal carcinoma in the lower quadrant of the left breast, Basal-like and axillary lymph node metastasis. a~c the lesion T2 shows high signal of lipid pressure, clear boundary, limited dispersion on DWI and ADC images,

and the ADC value is 0.86×10^{-3} mm²/s. e~f the DCE-MRI is unevenly reinforced, and the edge is ring reinforced, with an EER of 140.5% and TIC curve of type III

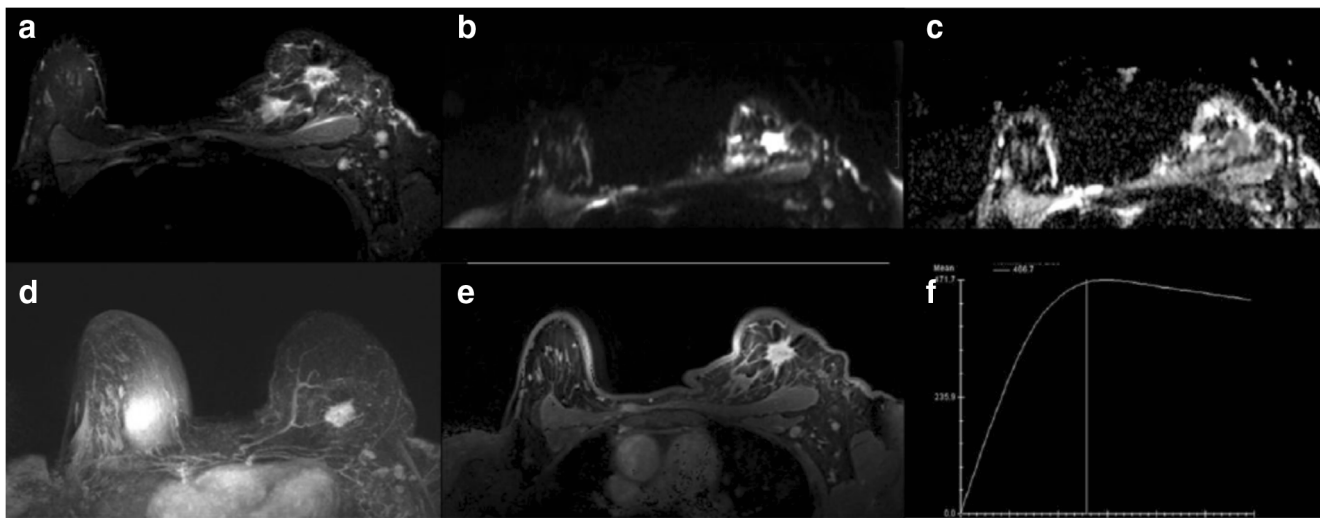


Fig. 3 Female patient, 39 years old, with a grade I infiltrating ductal carcinoma in the upper outer quadrant of the left breast, Luminal B and axillary lymph node metastasis. **a–c** the lesion T2 shows high signal of

lipid pressure, marginal burr, limited dispersion on DWI and ADC, and the ADC value is $0.98 \times 10^{-3} \text{ mm}^2/\text{s}$. **e–f** the DCE-MRI is unevenly reinforced, with an EER of 160% and a TIC curve of type III

discriminant functions of ADC value, EER, lobulation sign, burr sign, enhancement way, TIC in each model were obtained respectively. The discriminant results showed that the above indicators couldn't well predict the expression of immunohistochemical factors and molecular subtypes ($P < 0.05$), but they had a good prediction effect on pathological grade, with a false diagnosis rate of 9.69% ($X^2 = 2.033$, $P = 0.153$). The results were shown in Tables 6, 7 and 8.

Non-correlation between ADC values and molecular subtypes and prognostic factors

Cho et al. and Jeh et al. believed that the ADC value of ER and PR positive breast cancer was lower than that of the negative

group, and the ADC value of HER2+ breast cancer was higher than that of the negative group. In this study, there was no significant correlation between ADC value and molecular subtypes and immunohistochemical factors. The differences in the above research results may be related to the following factors: ER had the mechanism of inhibiting angiogenesis, which may reduce the microvascular perfusion of ER (+) breast cancer. Higher ADC values of ER (–) are associated with increased intratumoral microvascular perfusion effects; PR and HER2 can promote tumor microangiogenesis; ADC values were mixed with pure water molecular diffusion and microvasculature; the double information such as perfusion was different from the measured result; there were differences in research methods and samples. In addition, the results of

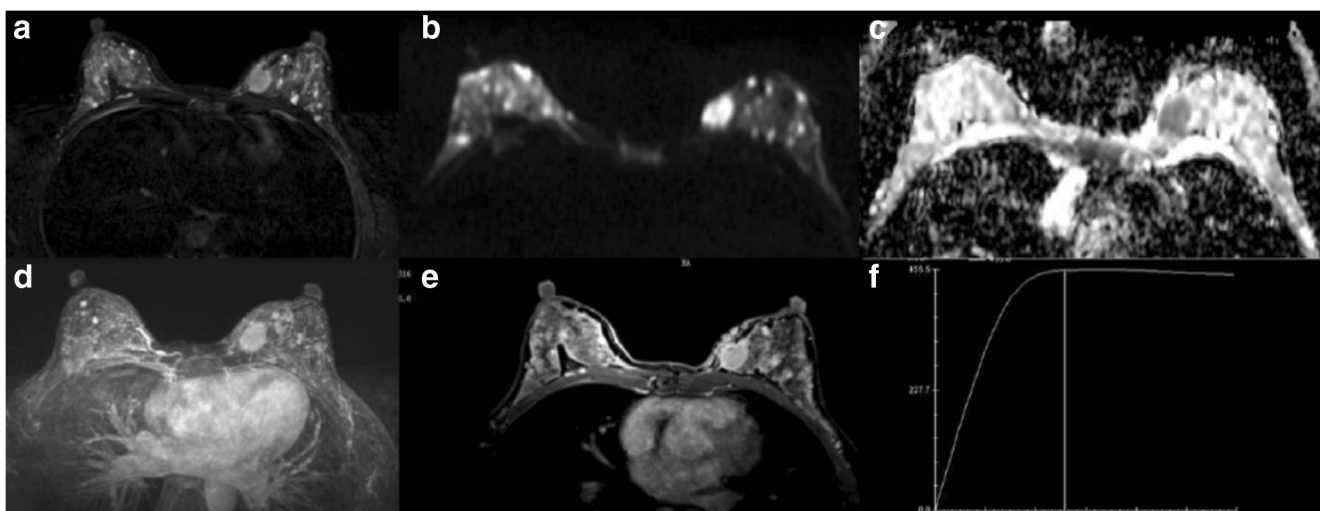


Fig. 4 Female patient, 56 years old, with a grade 3 infiltrating ductal carcinoma in the the inner quadrant of the left breast, HER2 overexpression and no axillary lymph node metastasis. **a–c** the lesion T2 shows high signal of lipid pressure, clear boundary, limited

dispersion on DWI and ADC images. **e–f** the DCE-MRI is unevenly reinforced, the ADC value is $0.78 \times 10^{-3} \text{ mm}^2/\text{s}$, with an EER of 140.5% and a TIC curve of type II

Table 3 Comparison of tumor size, lobulation, burr and other morphological features among groups of immunohistochemical factors

Immunohistochemical factor	Size (cm)	P value	Lobulation		P value	Burr		P value
			Yes	No		Yes	No	
ER								
Positive (145)	2.5 (2.0, 3.3)	0.001*	105	40	0.053	115	30	0.001*
Negative (51)	3.2 (2.4, 4.2)		37	14		26	25	
PR								
Positive (134)	2.6 ± 1.1	0.001*	98	36	0.061	107	27	0.001*
Negative (62)	3.4 ± 1.4		46	16		34	28	
HER2								
Positive (63)	3.2 (2.3, 4.0)	0.034*	51	12	0.667	44	19	0.655
Negative (133)	2.4 (2.0, 3.2)		111	22		97	36	
Ki67								
High (143)	2.6 (2.2, 3.5)	0.023*	120	23	0.446	65	78	0.009*
Low (53)	2.4 (1.7, 3.0)		42	11		43	10	

Mann-Whitney U test is used for comparison of size between groups; the differences between the lobulations and burrs are measured with a fourfold table chi-square test

*represents $P < 0.05$

this study showed that the ADC values of the high pathological grade and the lymph node metastasis groups were lower than the low pathological grade and the lymph node metastasis groups, which was negatively correlated ($r = -0.265 - 0.177$), consistent with most studies.

Correlation between tumor size and expression of immunohistochemical factors

Tumor size is a relatively valuable prognostic factor. The larger the tumor, the wider the infiltration range, the higher the risk of distant metastasis, and the poor the prognosis. Uma et al. and Kourea et al. found that the tumor volumes of the patients with negative PR and ER expressions and those with three negative expressions were significantly larger than that of the patients with positive expressions. The results of this study were basically consistent with those of Uma and Kourea. In

addition, the positive HER2 group was larger than the negative group (3.2 cm VS 2.4 cm, $P = 0.001$), while the tumor size of the HER2 overexpression was not significantly different from that of the Basal like (3.5 cm VS 3.2 cm, $P = 0.241$). Its pathological basis may be related to HER2 overexpression by inhibiting tumor cell apoptosis, inducing tissue angiogenesis, thereby promoting tumor growth, invasion and metastasis.

Enhancement ways

The enhancement ways of breast lesions are an important reference index in the differential diagnosis of benign and malignant lesions. Irregular morphology, uneven enhancement and ring enhancement are common signs of breast cancer. Among them, uneven or marginal enhancement is common in high grade invasive breast cancer. Batzer et al. found

Table 4 Comparison of tumor size, lobulation, burr and other morphological features between groups of molecular subtypes

Molecular subtype	Size (cm)	P value	Lobulation		P value	Burr		Burr
			Yes	No		Yes	No	
Luminal (148)	2.5 (2.0, 3.2)	0.018	128	20	0.008	116	32	0.013
vs								
HER2 overexpression (30)	3.5 (2.5, 4.6)		20	10		17	13	
Luminal (148)	2.5 (2.0, 3.2)	0.045	128	20	0.321	116	32	0.003
vs								
Basal-like (18)	3.2 (2.4, 3.6)		14	4		8	10	
HER2 (30)	3.5 (2.5, 4.6)	0.241	20	10	0.421	17	13	0.412
vs								
Basal-like (18)	3.2 (2.4, 3.6)		14	4		8	10	

Table 5 Correlation analysis of DCE-MRI features, ADC values, prognostic factors and molecular subtypes

Prognostic factor and molecular subtype	Correlation coefficient	Size	Lobulation	Burr	Reinforcement ways	TIC	EER (%)	ADC value
Pathological grade	r	0.144	0.264**	0.152	0.061	0.287**	0.168*	-0.265**
	p	0.073	0.001	0.054	0.401	0.001	0.019	0.001
Axillary lymph node metastasis	r	0.233**	0.185**	0.115	0.179*	0.095	0.149*	-0.177*
	p	0.003	0.009	0.109	0.012	0.187	0.037	0.013
ER	r	-0.289	0.147	0.298**	-0.035	-0.089	0.088	0.136
	p	0.001	0.053	0.001	0.630	0.213	0.220	0.405
PR	r	-0.297**	0.171	0.308**	-0.183**	-0.088	0.068	-0.051
	p	0.001	0.061	0.001	0.010	0.222	0.345	0.480
HER2	r	0.247**	0.031	0.032	0.110	0.228**	0.067	0.130
	p	0.001	0.667	0.655	0.125	0.001	0.352	0.178
Ki67	r	0.162	0.062	-0.185**	0.212**	0.038	0.086	0.053
	p	0.023	0.446	0.009	0.003	0.159	0.231	0.461
Molecular subtype	r	0.273**	-0.103	-0.235**	0.139	0.083	-0.053	0.060
	p	0.001	0.153	0.001	0.054	0.248	0.459	0.405

*indicates that the correlation is significant at the level of 0.05 (double-tailed)

**indicates that the correlation is significant at the level of 0.01 (double-tailed)

that edge enhancement was negatively correlated with expression of ER and PR and positively correlated with high expression of Ki67, and Boné et al. also obtained similar results. This study indicated that uneven enhancement or ring enhancement was negatively correlated with PR (+) and positively correlated with high expression of Ki67 and molecular subtype, and the results were consistent with the literature. The pathological basis was as follows: the growth rate of high grade tumor was fast, the nutrition in the tumor was unbalanced, and the central necrosis or multi-focal mixed necrosis area appeared; MVD was abundant in the edge area of the lesion in high grade breast cancer, which was significantly higher than the core area; the core area of breast cancer lesions can be dormant or fibrotic due to insufficient nutrient supply.

TIC and EER

Time-signal curve is a non-parametric index reflecting the blood perfusion and outflow rate of breast cancer lesions. Among them, the type III curve has higher predictive value for malignant lesions, while the early enhancement rate of malignant lesions is higher than that of benign lesions. TIC type was positively correlated with pathological grade and

proliferative activity of breast cancer. In invasive breast type III curve lesions, about 80% showed high proliferative activity, and high grade breast cancer has a higher early enhancement rate and outflow rate. The correlation analysis in this study showed that EER was positively correlated with pathological grade, TIC type was positively correlated with positive expression of HER2 and pathological grade, which was roughly consistent with the results of the previous literature.

The predictive value of DWI and DCE-MRI imaging parameters for prognostic factors and molecular subtypes

Bayesian discriminant analysis model was established for pathological grade, axillary lymph node metastasis, immunohistochemical factors and molecular subtypes. The discriminant results showed that ADC value, EER, lobulation sign, burr sign, enhancement way, TIC and other parameters couldn't predict the expression of immunohistochemical factors and molecular subtypes well (Tables 4, 5 and 6). However, the above indicators had a good effect on the prediction of pathological grade, with a total error rate of 9.69% ($X^2 = 2.033$, $P = 0.153$). Therefore, DWI and DCE-MRI are

Table 6 Bayesian discriminant analysis of molecular subtypes

Molecular subtype	Luminal A	Luminal B	HER2 overexpression	Basal-like
Actual classification	28	110	30	18
Discriminant classification	16	163	13	4

$X^2 = 28.874$, $P = 0.000 < 0.05$, indicating that the discriminant classification result is different from the actual classification result and the prediction effect is poor

Table 7 Bayesian discriminant analysis results of immunohistochemical factors

Immunohistochemical factor	ER		PR		HER2		Ki67	
	(+)	(-)	(+)	(-)	(+)	(-)	(+)	(-)
Actual classification	145	51	134	62	63	133	142	54
Discriminant classification	174	22	166	30	24	172	54	17
X^2	14.156		14.543		22.469		23.546	
<i>P</i>	0.000		0.001		0.000		0.000	

P < 0.05 indicates that the discriminant classification result is different from the actual classification result and the prediction effect is poor

not feasible in predicting immunohistochemical factors and molecular subtypes, but they have the potential to distinguish between high and low pathological grades.

Correlation between diffusion imaging parameters of breast cancer and biological prognostic factors

The ADC value of tissues is mainly affected by the diffusion of water molecules and microvascular perfusion in tissues. And the diffusion of water molecules is mainly affected by the restriction of biofilm structure and the adsorption of water molecules by macromolecular substances (such as proteins). The density of malignant breast tumor cells is high, and the diffusion of water molecules is significantly limited, resulting in a significantly reduced ADC value. Benign tumor blood vessels are less than malignant tumors, the proliferation of cells is slow, the density of parenchymal cells is low, the interstitial components are large, and the diffusion limitation of large water molecules in the extracellular space is low. Therefore, the ADC value decreases slightly, and the average ADC value is higher than that of malignant breast tumors. Some scholars found that ADC value was slightly negatively correlated with PCNA and p53 expression. PCNA is an indicator to evaluate tumor proliferation activity. The more vigorous the cell proliferation is, the higher the PCNA expression is, which conforms to the explanation that the more active the cell proliferation is, the lower the ADC value is. In this study, the expression of PCNA and p53 was not involved in

Table 8 Bayesian discriminant analysis results of pathological grade and axillary lymph node metastasis

Immunohistochemical factor	Pathological grade		Axillary lymph node metastasis	
	High grade	Low grade	Yes	No
Actual classification	178	18	114	82
Discriminant classification	169	27	143	53
X^2	2.033		9.502	
<i>P</i>	0.153*		0.002	

* represents *P* > 0.05, indicating that the discriminant classification result is roughly the same as the actual classification result, and the prediction effect is good

immunohistochemical staining in 104 breast cancer patients. Calvar et al. found that the ADC value of brain tumors was negatively correlated with the expression of Ki-67 marker index, that is, the higher the Ki-67 marker index is, the more vigorous the tumor cell proliferation is and the lower the ADC value is. In this study, there was no correlation between the ADC value and the expression of biological prognostic factors, and the ADC value couldn't be used to predict the expression of biological prognostic factors of breast cancer.

Conclusion

Imaging examination method, image analysis, post-processing method, pathological results, molecular typing method, and DWI imaging technology were used to analyze the correlation between DWI and DCE-MRI imaging features of breast cancer and molecular subtypes and prognostic factors. It was found that parameters such as ADC value, EER, lobulation sign, burr sign, enhancement way, TIC type and so on were correlated with prognostic factors and molecular subtypes. And Bayesian model discriminant analysis showed that the above imaging parameters couldn't well predict the expression of immunohistochemical factors and molecular subtypes. However, the above characteristics had a good effect on the prediction of pathological grade, with a false diagnosis rate of 9.69%, indicating that DWI and DCE-MRI were not feasible in predicting the expression of immunohistochemical factors and molecular subtypes of breast cancer, but they were of high value in identifying the high and low pathological grades of breast cancer, and could be applied in the early pathological remission evaluation of neoadjuvant chemotherapy for breast cancer.

Compliance with Ethical Standards

Conflict of Interest Author Congru Yuan declares that he has no conflict of interest. Author Feng Jin declares that he has no conflict of interest. Author Xiuling Guo declares that he has no conflict of interest. Author Sheng Zhao declares that he has no conflict of interest. Author Wei Li declares that he has no conflict of interest. Author Haidong Guo declares that he has no conflict of interest.

Ethical Approval All procedures performed in studies involving human participants were in accordance with the ethical standards of the institutional and/or national research committee and with the 1964 Helsinki declaration and its later amendments or comparable ethical standards.

This article does not contain any studies with animals performed by any of the authors.

Informed Consent Informed consent was obtained from all individual participants included in the study.

Publisher's Note Springer Nature remains neutral with regard to jurisdictional claims in published maps and institutional affiliations.

References

1. Savas, P., Salgado, R., and Denkert, C., Clinical relevance of host immunity in breast cancer: From TILs to the clinic. *Nat. Rev. Clin. Oncol.* 13(4):228, 2016.
2. Bianchini, G., Balko, J. M., and Mayer, I. A., Triple-negative breast cancer: Challenges and opportunities of a heterogeneous disease. *Nat. Rev. Clin. Oncol.* 13(11):674, 2016.
3. Ogino, S., Nishihara, R., and VanderWeele, T. J., The role of molecular pathological epidemiology in the study of neoplastic and non-neoplastic diseases in the era of precision medicine. *Epidemiology (Cambridge, Mass.)* 27(4):602, 2016.
4. Yang, L., Feng, Y., Qi, P., Xu, S., and Zhou, Y., Mechanism of serum miR-21 in the pathogenesis of familial and triple negative breast cancer. *J. Biol. Regul. Homeost. Agents* 30(4):1041–1045, 2016.
5. Li, M. L., Dong, Y., Luan, S. L., Zhao, Z. H., and Ning, F. L., Changes of expression of estrogen and progesterone receptors, human epithelial growth factor receptor 2 and Ki-67 after neoadjuvant chemotherapy in the treatment of breast cancer. *J. Biol. Regul. Homeost. Agents* 30(4):1059–1065, 2016.
6. Pichler, M., Stiegelbauer, V., and Vychytilova, F. P., Genome-wide miRNA analysis identifies miR-188-3p as a novel prognostic marker and molecular factor involved in colorectal carcinogenesis. *Clin. Cancer Res.* 23(5):1323–1333, 2017.
7. Wang, Y., Cao, C., Fang, D., and Hu, Y., Role of APC-mediated MDR-1/CLCX-1 signaling pathway in ovarian tumors. *J. Biol. Regul. Homeost. Agents* 32(3):529–536, 2018.
8. Hendry, S., Salgado, R., and Gevaert, T., Assessing tumor-infiltrating lymphocytes in solid tumors: A practical review for pathologists and proposal for a standardized method from the international Immuno-oncology biomarkers working group: Part 2: TILs in melanoma, gastrointestinal tract carcinomas, non-small cell lung carcinoma and mesothelioma, endometrial and ovarian carcinomas, squamous cell carcinoma of the head and neck, genitourinary carcinomas, and primary brain tumors. *Adv. Anat. Pathol.* 24(6):311–335, 2017.
9. Pesapane, F., Patella, F., and Fumarola, E. M., Intravoxel incoherent motion (IVIM) diffusion weighted imaging (DWI) in the periferic prostate cancer detection and stratification. *Med. Oncol.* 34(3):35, 2017.
10. Lee, P., Ryoo, H., and Park, J., Morphological and microstructural changes of the hippocampus in early MCI: A study utilizing the Alzheimer's disease neuroimaging initiative database. *J. Clin. Neurol.* 13(2):144–154, 2017.